Magnetic ordering and superconductivity in $R_2Rh_3Sn_5$ (R=La-Tm,Y) systems

N. G. Patil and S. Ramakrishnan
Tata Institute Of Fundamental Research, Bombay-400005, India
(Received 9 March 1998; revised manuscript received 6 November 1998)

We report resistivity, magnetization and heat-capacity studies on $R_2Rh_3Sn_5$ (R=La-Tm, Y) from 1.5 to 300 K. We find that $La_2Rh_3Sn_5$ forms in $U_2Co_3Si_5$ (*Ibam*) structure while the others (R=Ce to Tm) adopt the related $Y_2Rh_3Sn_5$ ($Cmc2_1$) structure. Both structures are closely related to the structure of $R_2Fe_3Si_5$ ($P4/mnc$) compounds which exhibit exotic superconducting and magnetic properties. $Ce_2Rh_3Sn_5$ shows a Kondo lattice behavior and undergoes antiferromagnetic ordering below 2.5 K whereas compounds $La_2Rh_3Sn_5$ and $Tm_2Rh_3Sn_5$ show superconductivity below 1.8 K. The observed superconductivity in $Tm_2Rh_3Sn_5$ is interesting in view of its bulk magnetic ordering below 2.3 K. The other compounds containing magnetic rare-earth elements undergo antiferromagnetic ordering at low temperatures ($T \leqslant 10$ K) with the exception of $Pr_2Rh_3Sn_5$ and $Nd_2Rh_3Sn_5$ which do not order down to 1.5 K. [S0163-1829(99)01618-5]

I. INTRODUCTION

Ternary silicides and germanides which form in a rich variety of crystal structures[1,2] exhibit unusual physical properties. A few of them undergo superconducting transition at low temperatures[3,4] while others show exotic magnetic ordering arising from RE^{3+} moments. Considerable efforts have been made to understand the superconductivity and magnetism observed in the compounds belonging to the $R_2Fe_3Si_5$ series.[5–8] It has been suggested that the Fe atoms do not carry any moment in the above series but help in building a large density of states at the Fermi level.[9] Previous studies have established that a member of this series, namely, $Tm_2Fe_3Si_5$,[10] is the first reentrant antiferromagnetic superconductor. It is worthwhile to point out that we still do not know why the antiferromagnetic order among Tm^{3+} ions is a deterrent to the superconductivity in $Tm_2Fe_3Si_5$ given that the neutron-scattering studies[10] could not find any ferromagnetic component in the magnetic unit cell in this compound. A recent investigation claims that an antiferromagnet $Er_2Fe_3Si_5$ (Ref. 11) (below 2.5 K) becomes superconducting below 1 K. Although many attempts have been made in $R_2Fe_3Si_5$ series, only very few investigations have been done to understand the superconductivity in other silicides and germanides.[12–14] In particular, we are aware of only three reports on the superconductivity and magnetism of $R_2Rh_3Si_5$ series[12,14,15] whose structure is closely related to $R_2Fe_3Si_5$ family. Several years ago, Meot-Meyer *et al.*[16] reported the formation of a series $R_2Rh_3Sn_5$ whose structure is closely related to that of $R_2Fe_3Si_5$ and $R_2Rh_3Si_5$ series. Although the crystal structures of these iron silicides, rhodium silicides, and rhodium stannides with rare earths are derived from $BaAl_4$-type structure, the iron silicides exist in the tetragonal structure (space group $P4/mnc$) while rhodium silicides and rhodium stannides form in orthorhombic structure albeit with different space groups, namely, *Ibam* and $Cmc2_1$, respectively. Since it is now well established that the compounds of $R_2Fe_3Si_5$ series exhibit unusual superconducting and magnetic properties, it will be of interest to study the magnetism and superconductivity in $R_2Rh_3Sn_5$ family. With this in view, as a part of our detailed study on this series, we report our resistivity, magnetization, and heat-capacity measurements on $R_2Rh_3Sn_5$ (R=Ce to Tm) from 1.5 to 300 K.

II. EXPERIMENTAL DETAILS

Samples of $R_2Rh_3Sn_5$ (R=Y, La to Tm) were made by melting the individual constituents (taken in stoichiometric proportions) in an arc furnace under high-purity argon atmosphere. The purity of the rare-earth metals and Rh was 99.9% whereas the purity of Sn was 99.999%. The alloy buttons were remelted five to six times to ensure proper mixing. The samples were annealed at 900 °C for a week. The x-ray powder-diffraction pattern of the samples did not show the presence of any parasitic impurity phases. All the samples except $La_2Rh_3Sn_5$ were found to adopt the orthorhombic $Y_2Rh_3Sn_5$ structure ($Cmc2_1$).[16] The lattice constants *a*, *b*, and *c* are given in Table I where they are seen to decrease across the series (i.e., from $Ce_2Rh_3Sn_5$ to $Tm_2Rh_3Sn_5$). The compounds with R=La, Ce, Pr, and Nd are synthesized in this work. However, the lattice constants determined for the remaining compounds are in close agreement with those published earlier by Meot-Meyer *et al.*[16] The compound $La_2Rh_3Sn_5$ forms with the orthorhombic $U_2Co_3Si_5$ (*Ibam*)

TABLE I. Structural properties of $R_2Rh_3Sn_5$.

Sample	a(Å)	b(Å)	c(Å)
$La_2Rh_3Sn_5$[a]	10.667±.005	12.891±.005	6.315±.005
$Ce_2Rh_3Sn_5$	4.506±.005	26.383±.005	7.212±.005
$Pr_2Rh_3Sn_5$	4.481±.005	26.444±.005	7.208±.005
$Nd_2Rh_3Sn_5$	4.467±.005	26.363±.005	7.205±.005
$Gd_2Rh_3Sn_5$	4.419±.005	26.132±.005	7.167±.005
$Tb_2Rh_3Sn_5$	4.402±.005	26.183±.005	7.140±.005
$Dy_2Rh_3Sn_5$	4.396±.005	26.188±.005	7.138±.005
$Ho_2Rh_3Sn_5$	4.380±.005	26.111±.005	7.132±.005
$Er_2Rh_3Sn_5$	4.355±.005	26.128±.005	7.132±.005
$Tm_2Rh_3Sn_5$	4.341±.005	26.198±.005	7.147±.005
$Y_2Rh_3Sn_5$	4.395±.005	26.151±.005	7.137±.005

[a]Different structure (see text).

structure. Both unit cells have 40 atoms but $Y_2Rh_3Sn_5$ has two distinct sites for Y whereas $U_2Co_3Si_5$ has only a single site for U. However, it must be remembered that the $U_2Co_3Si_5$ can be considered as an intergrowth of $CaBe_2Ge_2$-type slabs with slabs of composition RT_3 (R = rare earth, T = transitional metal).[17] The unit cell for $La_2Rh_3Sn_5$ has a single La site, two Rh sites, and three Sn sites. On the other hand, the $Y_2Rh_3Sn_5$ structure is essentially a three-dimensional lattice of Rh-Sn covalent bonds with two rare-earth sites, three Rh sites, and five Sn sites. Hence the net hybridization between d and f orbitals can be very different for these two structures which has to be taken into account in the analysis of magnetic ordering temperatures.

The temperature dependence of dc susceptibility (χ) was measured using Faraday method in a field of 4 kOe in the temperature range from 4–300 K. The ac susceptibility was measured using a home-built susceptometer[18] from 1.5–20 K. The absolute accuracy with which magnetization measurements were performed is within 1%. The resistivity was measured using a four-probe dc technique with contacts made using silver paint on a cylindrical sample of 2-mm diameter and 10-mm length. The temperature was measured using a calibrated Si diode (Lake Shore Inc., USA) sensor. The sample voltage was measured with a nanovoltmeter (model 182, Keithley, USA) with a current of 10 mA provided by a current source (Hewlett Packard, USA) with 20-ppm stability. All the data were collected using an IBM compatible PC/AT via IEEE-488 interface. The relative accuracy of the resistance measurements is 50 ppm while the accuracy of the absolute resistivity is only 5% due to errors in estimating the geometrical factors. The heat capacity in zero field from above 1.7–35 K was measured with an accuracy of 1% using an automated adiabatic heat-pulse calorimeter. A calibrated germanium resistance thermometer (Lake Shore Inc., USA) was used as the temperature sensor in this range.

III. RESULTS

A. Magnetic susceptibility and magnetization studies

1. Properties of $La_2Rh_3Sn_5$ and $Y_2Rh_3Sn_5$

The temperature dependence of the dc magnetic susceptibility (χ) of $La_2Rh_3Sn_5$ sample is shown in Fig. 1. The normal state χ of this sample has a weak temperature dependence with a value of 1.2×10^{-3} emu/mol at 300 K and reaches a value of 2.4×10^{-3} emu/mol at 10 K. Such a small temperature dependence of χ could be either intrinsic or extrinsic to the sample. The intrinsic reason could attributed to the temperature variation of density of states at the Fermi level which results in the temperature dependence of Pauli spin susceptibility as seen in some of the $A-15$ compounds.[19] On the other hand, such a temperature dependence could be caused by the presence of 900 ppm of Gd impurities (which could be paramagnetic) in the ''pure'' La used for making the sample. To settle this issue, one could do perturbed angular correlation (PAC) studies using Sn source or ^{14}Si NMR measurements to find whether the local susceptibility shows a temperature dependence which arises due to changes in the density of states at the Fermi level. The

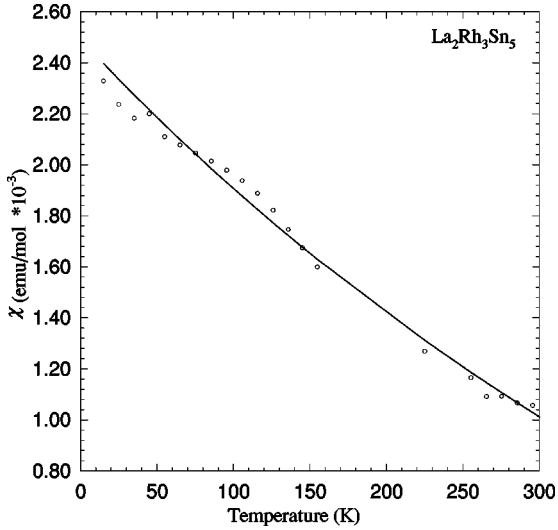

FIG. 1. Variation of susceptibility (χ) of $La_2Rh_3Sn_5$ from 5–300 K in 4 kOe. This variation could be extrinsic (impurity effects) or due to intrinsic effects such as the variation of density of state at the Fermi level. See text for details.

χ value of $Y_2Rh_3Sn_5$ at 300 K is 5×10^{-4} emu/mol which suggests smaller value of density of states at the Fermi level.

2. Properties of $R_2Rh_3Sn_5$ (R=Ce-Tm)

The temperature dependence of the inverse dc magnetic susceptibility (χ^{-1}) of $R_2Rh_3Sn_5$ (R=Ce, Pr, Nd, and Gd) is shown in Fig. 2. Similar data for R=Tb, Dy, Ho, Er, and Tm are shown in Fig. 3. Insets show the low-temperature χ behavior of the respective compounds. The high-temperature susceptibility ($100<T<300$ K) is fitted to a modified Curie-Weiss expression which is given by

$$\chi=\chi_0+\frac{C}{(T-\theta_p)}, \tag{1}$$

where C is the Curie constant which can be written in terms of the effective moment as

$$C(\text{emu K/mol})\approx\frac{\mu_{\text{eff}}(\mu_B)^2x}{8}, \tag{2}$$

where x is the number of magnetic R ions per formula unit. The values of χ_0, μ_{eff}, and θ_p are given in Table II. The main contributions to the temperature independent χ_0 are namely the diamagnetic susceptibility which arises due to the presence of ion cores and the Pauli spin susceptibility of the conduction electrons. The estimated effective moment in many cases is found to be smaller than the free ion moment of RE^{3+} ion which could be due to the presence of crystal-field effects in these compounds. Negative value of the Curie-Weiss temperature (θ_p) implies the presence of antiferromagnetic correlations while positive θ_p could indicate ferromagnetic correlations at high temperatures. From Table II, one can notice that only θ_p of both Gd- and Tm-based compounds show positive values. Large value of θ_p in $Ce_2Rh_3Sn_5$ implies the role of strong hybridization of $5f$ orbitals of Ce while high positive value of θ_p in $Tm_2Rh_3Sn_5$ is quite puzzling. However, we wish to recall here that the

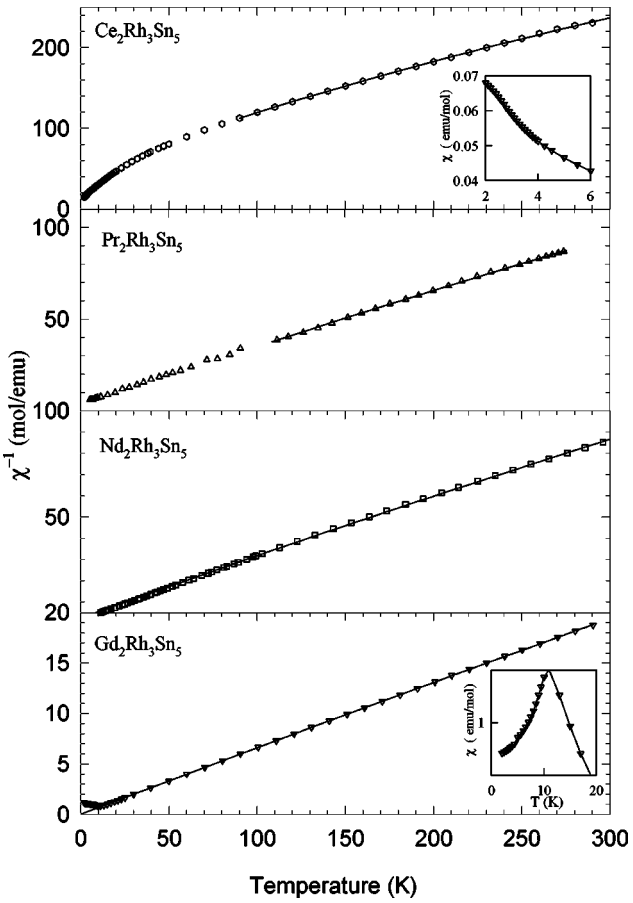

FIG. 2. Variation of inverse dc susceptibility ($1/\chi$) of $R_2Rh_3Sn_5$ (R=Ce, Pr, Nd, and Gd) from 3–300 K in a field of 4 kOe. The inset shows the χ behavior at low temperatures. The solid line is a fit to the Curie-Weiss relation (see text for details).

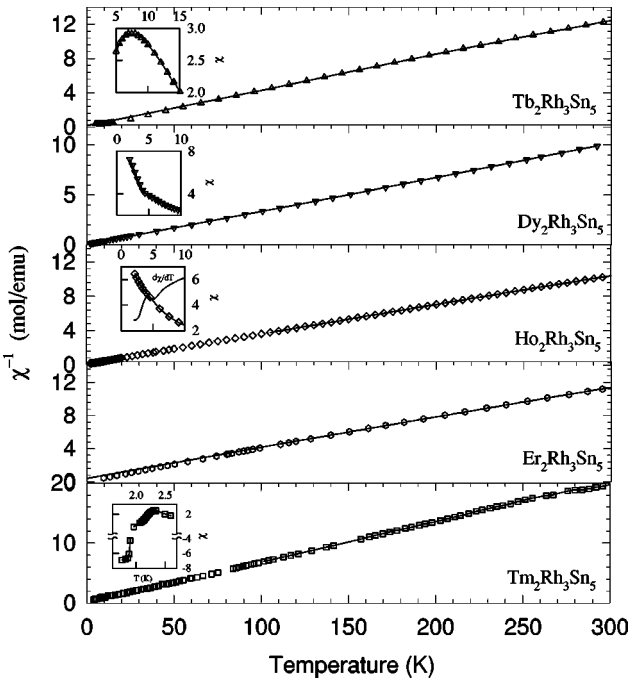

FIG. 3. Variation of inverse dc susceptibility ($1/\chi$) of $R_2Rh_3Sn_5$ (R=Tb, Dy, Ho, Er, and Tm) from 3–300 K in a field of 4 kOe. The insets show χ behavior at low temperatures. The solid line is a fit to the Curie-Weiss relation (see text for details).

measurements were made on polycrystals so anisotropy could play an important role here. Complete analysis awaits studies on single crystals of these samples. The low-temperature data show a change of slope in χ at 4 K which we identify as the ordering temperature of this compound. The low-temperature behavior of $\chi(T)$ of $Tm_2Rh_3Sn_5$ vividly demonstrates the antiferromagnetic ordering of Tm^{3+} moments at 2.3 K and the superconductivity at 1.8 K which is exemplified by the diamagnetic transition below 1.8 K. Our ac susceptibility measurements (not presented here) are in agreement with this result. The transition temperatures of various compounds obtained from magnetic susceptibility measurements are listed in Table III.

3. Magnetization studies of $R_2Rh_3Sn_5$ (R=Ce, Gd, Dy, and Ho)

Isothermal magnetization measurements at various temperatures on some of the samples of the series $R_2Rh_3Sn_5$ are shown in Fig. 4. Non-linear behavior in M vs H at the lowest temperature agrees with the notion of antiferromagnetic ordering of Ce^{3+} and Gd^{3+} spins. This non-linear behavior persists up to 10 K in the case of the Gd compound and 5 K for the Ce one. At higher temperatures (T=25 K>T_N), one observes usual linear behavior in magnetization which characterizes the paramagnetic state. The magnetization values of Ce are very small presumably due to the presence of Kondo effect. On the other hand, the magnetization data of Dy and Ho show large moments with possible metamagnetic transitions at 3 K. The nonlinearity in M vs H above T_N in the case of Tb and Dy could arise due to the splitting of energy levels by crystalline electric field (CEF). More investigations such as neutron-scattering (elastic and inelastic) measurements are essential to solve the magnetic structures and CEF levels of these compounds.

B. Resistivity studies of $R_2Rh_3Sn_5$ (R=La-Tm, Y)

The resistivity data (ρ) of $R_2Rh_3Sn_5$ (R=La-Tm, Y) series are shown in Fig. 5 and Fig. 6. The insets (for all compounds except R=Ce and Y) show the low-temperature ρ data on an expanded scale. The ρ data of $La_2Rh_3Sn_5$ show a

TABLE II. Parameters obtained from the high-temperature susceptibility fit to the Curie-Weiss expression given by Eq. (1). μ_{th} is theoretical free ion value.

Sample	χ_0	μ_{eff}	μ_{th}	θ_p
$La_2Rh_3Sn_5$	-3.76×10^{-3}	-	-	-
$Ce_2Rh_3Sn_5$	106×10^{-3}	2.109	2.54	−52
$Pr_2Rh_3Sn_5$	1.058×10^{-3}	3.414	3.58	−5.4
$Nd_2Rh_3Sn_5$	7.73×10^{-4}	3.65	3.62	−8.2
$Gd_2Rh_3Sn_5$	1.81×10^{-3}	7.72	7.94	0.34
$Tb_2Rh_3Sn_5$	9.25×10^{-4}	9.14	9.7	−7.4
$Dy_2Rh_3Sn_5$	-1.68×10^{-3}	10.92	10.65	−1.47
$Ho_2Rh_3Sn_5$	3.6×10^{-3}	10.56	10.61	−1.02
$Er_2Rh_3Sn_5$	3.8×10^{-3}	10.2	9.59	−9.98
$Tm_2Rh_3Sn_5$	7.5×10^{-3}	6.98	7.56	14.57
$Y_2Rh_3Sn_5$	2.9×10^{-4}	-	-	-

TABLE III. Transition temperatures T_p (T_N or/and T_c) obtained from different measurement techniques. These transitions are determined from the slope change in their respective properties as a function of temperature. Most of them are T_N values except for La and Tm compounds.

Sample	T_p(K) Resistivity	Susceptibility	Heat capacity
$La_2Rh_3Sn_5$	1.85 K[a]	1.8 K[a]	1.8 K[a]
$Ce_2Rh_3Sn_5$	5 K	4 K	2.5 K
$Gd_2Rh_3Sn_5$	10.0 K	10.0 K	10.0 K
$Tb_2Rh_3Sn_5$	−,7.0 K	4.0 K, 6.0 K	4.0 K, 6.3 K
$Dy_2Rh_3Sn_5$	−,6.5 K	4.0 K,−	4.0 K, 6.0 K
$Ho_2Rh_3Sn_5$	4.5 K	5.0 K	5.0 K
$Er_2Rh_3Sn_5$	3.2 K	−	2(onset) K
$Tm_2Rh_3Sn_5$	2.3 K, 1.8 K[a]	2.3 K, 1.8 K[a]	2.3 K,−

[a]Superconducting transition (T_c).

sharp jump at 1.85 K which is the superconducting transition temperature (T_c) of this sample. We found the value of the transition width (ΔT_c) to be 0.1 K. A similar superconducting transition at 1.8 K is observed in $Tm_2Rh_3Sn_5$ which also shows antiferromagnetic ordering below 2.3 K. For those samples which undergo magnetic transitions in the temperature range of our measurements, the resistivity data exhibit a change of slope which can be used as an alternative estimate of Néel temperature. However, the change of slope in the resistivity data of $Pr_2Rh_3Sn_5$ around 2.5 K is attributed to the CEF since neither ac susceptibility nor heat capacity shows ordering down to 1.5 K. Such an anomaly often occurs in praseodymium compounds due to a singlet ground state arising from CEF splitting of $(2J+1)$ levels of the non-Kramers Pr^{3+} ion.

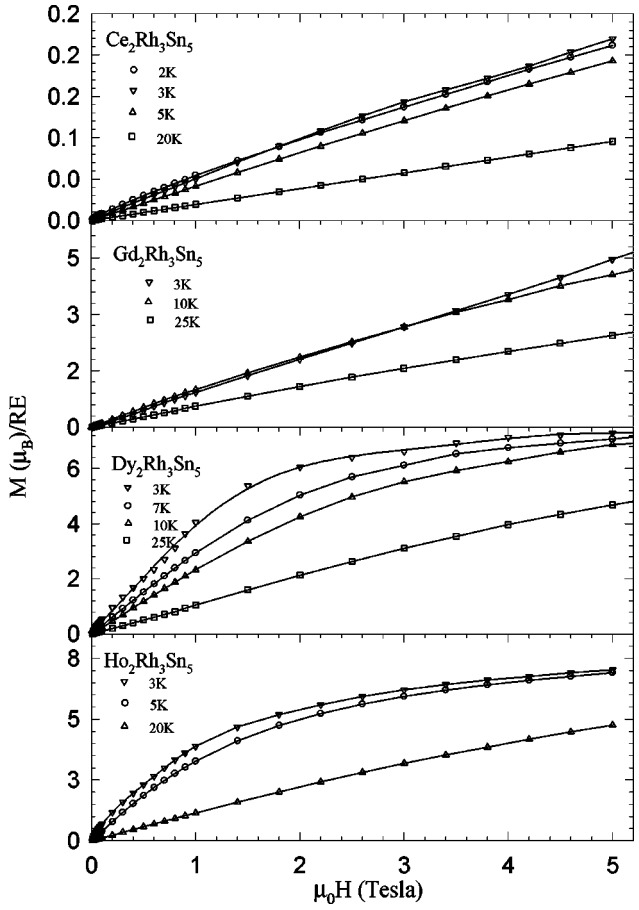

FIG. 4. Isothermal magnetization (M) of $R_2Rh_3Sn_5$ (R=Ce, Gd, Dy, and Ho) vs magnetic field (H) at various temperatures. The nonlinearity in M vs H at the lowest temperature agrees with the notion of antiferromagnetic ordering of RE^{3+} spins whereas the linear dependence of M on H at 25 K signifies that the sample is in the paramagnetic state at this temperature.

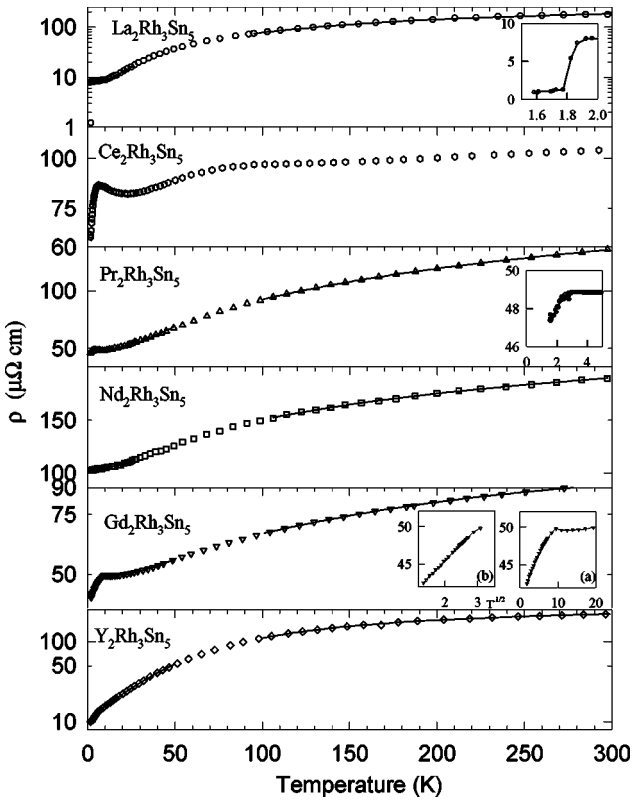

FIG. 5. Temperature dependence of resistivity (ρ) of $R_2Rh_3Sn_5$ (R=La, Ce, Pr, Nd, Gd, and Y) from 1.5–300 K. The insets show the low-temperature ρ data. The solid lines in the main panel are fit to the model (see text). For $Gd_2Rh_3Sn_5$, inset (b) shows $T^{\frac{1}{2}}$ dependance at low temperature.

In the normal state, the low-temperature dependence of ρ could be fitted to a power law which can be written as

$$\rho = \rho_0 + aT^n. \tag{3}$$

The values of ρ_0, a, and n are given in Table IV. For $La_2Rh_3Sn_5$ and $Y_2Rh_3Sn_5$, the optimum value of n is found to be 2.5 and 1.5, respectively. These values disagree with Wilson's s-d scattering model which predicts a T^3 dependence of $\rho(T)$ for $T<\theta_D/10$. However, the low-temperature resistivity exhibits a power-law dependence with $n<3$ in many nonmagnetic rare-earth intermetallic alloys. Such a discrepancy could arise due to a variety of reasons such as complex structure of the Fermi surface, phonon-drag effects, and lattice anharmonicity.

The ρ of most of the magnetic rare-earth samples shows a T^2 dependence in the low-temperature paramagnetic region ($T_N<T<25$ K) with the exception of compounds made from Ce, Er, and Tm. Figure 5 shows the temperature dependence

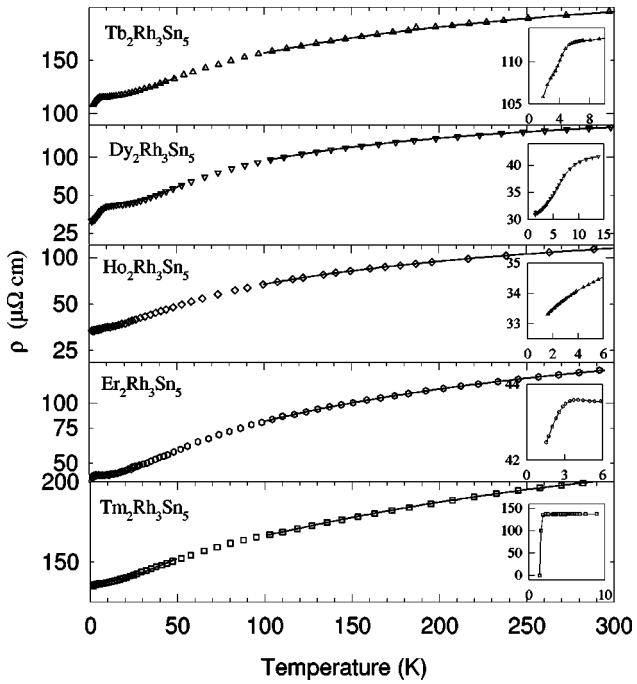

FIG. 6. Temperature dependence of resistivity (ρ) of $R_2Rh_3Sn_5$ (R=Tb, Dy, Er, Ho, and Tm) from 1.5–300 K. The insets show the low-temperature ρ data. Note that the Tm sample undergoes superconducting transition below 2 K. The solid lines in the main plot are fit to the model (see text).

of ρ of $Ce_2Rh_3Sn_5$ from 1.5–300 K. The decrease of ρ with temperature above T_N agrees with the notion of the presence of Kondo effect in this sample. This is in agreement with our magnetization measurements where we observed reduced moment for Ce^{3+} ion. The inset in the resistivity data of $Ce_2Rh_3Sn_5$ shows the magnetic contribution to ρ which displays Kondo-like response. However, ρ of $Er_2Rh_3Sn_5$ shows a $T^{2.5}$ dependence while that of $Tm_2Rh_3Sn_5$ exhibits a $T^{1.5}$ dependence. Why the ρ at low temperature of these two compounds (Er and Tm) show a different power-law dependence is not understood at present. The resistivity data of $Gd_2Rh_3Sn_5$ between 1.5 and T_N=10 K show $T^{1/2}$ dependence which is different from the usual dependence of ρ (T^n with $n>1$) expected below the antiferromagnetic ordering.

TABLE IV. Parameters obtained from the low temperature resistivity fit in $R_2Rh_3Sn_5$.

Sample	ρ_0 $\mu\Omega$ cm	a $n\Omega$ cm/K^n	n n
$La_2Rh_3Sn_5$	8.17	2.57	2.5
$Pr_5Rh_3Sn_5$	48.6	6.67	2
$Nd_5Rh_3Sn_5$	103	10.4	2
$Gd_2Rh_3Sn_5$	48.6	2.59	2
$Tb_2Rh_3Sn_5$	112	7.86	2
$Dy_2Rh_3Sn_5$	38.9	7.48	2
$Ho_2Rh_3Sn_5$	33.7	43.9	2
$Er_2Rh_3Sn_5$	43.4	1.27	2.5
$Tm_2Rh_3Sn_5$	138	38.4	1.5
$Y_2Rh_3Sn_5$	12.3	113	1.5

A brief account of how such a $T^{1/2}$ dependence can be attributed to the scattering of conduction electrons by critical spin fluctuations that occur near T_N will be given in the discussion section. In the case of $Tb_2Rh_3Sn_5$, a distinct change of slope in low-temperature resistivity data is seen at 4 and 6 K. We believe these changes of slope probably represent two magnetic transitions in this sample. However, from the ρ data of $Dy_2Rh_3Sn_5$, we could discern only a single transition while heat-capacity data show two transitions. The transition temperatures observed from resistivity data are compared with those obtained from susceptibility and heat-capacity studies (described later) in Table III.

At high temperatures ($100<T<300$ K), the resistivity data deviate significantly from the expected linear temperature dependence. This has been seen in many compounds where the value of ρ becomes sufficiently large for the mean free path to shorten to the order of a few atomic spacings. When that happens, the scattering cross section will no longer be linear in the scattering perturbation. Since the dominant temperature-dependent scattering mechanism is electron-phonon interaction here, the ρ will no longer be proportional to the mean-square atomic displacement, which is proportional to T for a harmonic potential. Instead, the resistance will rise less rapidly than linearly in T and will show negative curvature ($d^2\rho/dT^2<0$). This behavior was also seen in previous studies on silicides and germanides.[20,21]

One of the models which describe the $\rho(T)$ of these compounds is known as the parallel resistor model.[22] In this model the expression of $\rho(T)$ is given by

$$\frac{1}{\rho(T)}=\frac{1}{\rho_1(T)}+\frac{1}{\rho_{max}}, \tag{4}$$

where ρ_{max} is the saturation resistivity which is independent of temperature and $\rho_1(T)$ is the ideal temperature-dependent resistivity. Further, the ideal resistivity is given by the following expression:

$$\rho_1(T)=\rho_0+C_1\left(\frac{T}{\theta_D}\right)^3\int_0^{\theta_D/T}\frac{x^3dx}{[1-\exp(-x)][\exp(x)-1]}, \tag{5}$$

where $\rho(0)$ is the residual resistivity and the second term is due to phonon-assisted electron scattering similar to the s-d scattering in transition metal compounds. θ_D is the Debye temperature and C_1 is a numerical constant. Equation (4) can be derived if we assume that the electron mean free path l is replaced by $l+a$ (a being an average interatomic spacing). Such an assumption is reasonable, since infinitely strong scattering can only reduce the electron mean free path to a. Chakraborty and Allen[23] have made a detailed investigation of the effect of strong electron-phonon scattering within the framework of the Boltzmann transport equation. They find that the interband scattering opens up new *nonclassical channels* which account for the parallel resistor model. The high temperature ($100<T<300$ K) ρ data of all the samples could be fitted to the parallel resistor model. The values of the various parameters obtained from the fit to this model are listed in Table V. The observed θ_D values from the heat-capacity data (discussed below) are also given in Table V.

TABLE V. Parameters obtained from the fit of the high-temperature data to the parallel resistor model in $R_2Rh_2Sn_5$. θ_D(obs) is the observed value from heat-capacity studies.

Sample	ρ_{max} $\mu\Omega$ cm	ρ_0 $\mu\Omega$ cm	C_1 $\mu\Omega$cm	θ_D(fit) K	θ_D(obs) K
$La_2Rh_3Sn_5$	374	49	1264	531	190
$Pr_2Rh_3Sn_5$	500	82	576	481	333
$Nd_2Rh_3Sn_5$	364	183	617	299	201
$Gd_2Rh_3Sn_5$	144	97	627	525	244
$Tb_2Rh_3Sn_5$	368	203	780	342	248
$Dy_2Rh_3Sn_5$	359	59	595	310	230
$Ho_2Rh_3Sn_5$	292	58	328	356	267
$Er_2Rh_3Sn_5$	541	64	339	345	175
$Tm_2Rh_3Sn_5$	321	294	850	469	185
$Y_2Rh_3Sn_5$	338	26	1535	355	222

No attempt was made to fit the parallel resistor model to that ρ data of $Ce_2Rh_3Sn_5$ since this compound exhibits Kondo behavior.

C. Heat capacity studies of $R_2Rh_3Sn_5$ (R=La-Tm)

The temperature dependence of the heat-capacity (C_p) of various compounds of the series $R_2Rh_3Sn_5$ is shown in Fig. 7 and Fig. 9. For those samples with magnetic RE ions, the magnetic contribution to the entropy, S_{mag}, is included as a broken curve. The magnetic entropies at 35 K and (where appropriate) at T_N are listed in Table VI where they are given per mol of RE ion and are normalized against the gas constant (R). Fig. 8 and the insets of Fig. 7 show the low temperature C_p/T vs T^2 data.

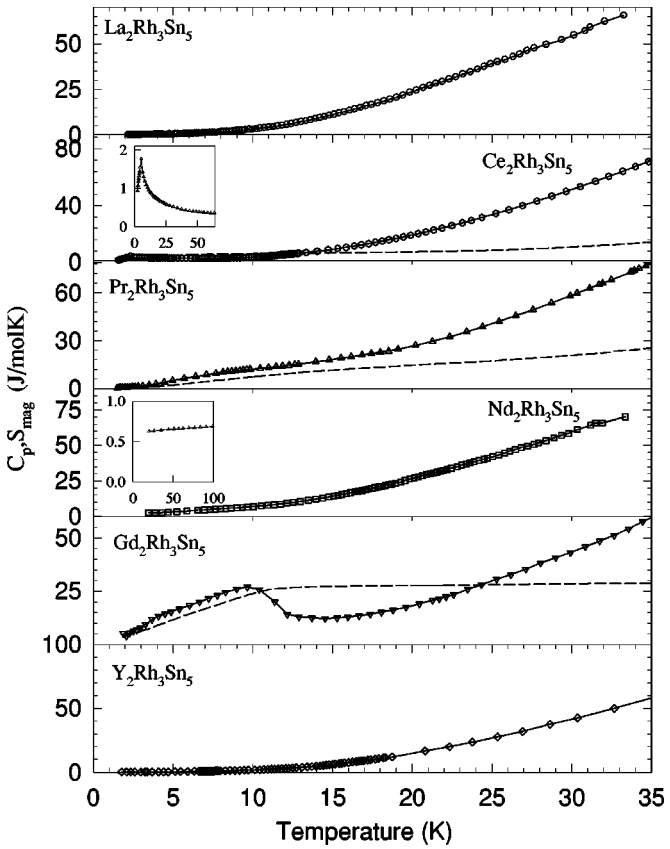

FIG. 7. Temperature dependence of the heat capacity (C_p) of $R_2Rh_3Sn_5$ (R=La, Ce, Pr, Nd, Gd, and Y). The insets show low-temperature C_p/T vs T^2 data. The calculated values entropy S_{mag} (after the subtraction of the lattice contribution from C_p) are also given.

TABLE VI. Parameters obtained from the heat-capacity measurements in $R_2Rh_3Sn_5$.

Sample	T_N(K)	S($T_N{}^b$)/R	J	ln(2J+1)	S_{mag}(35 K)/R
$Ce_2Rh_3Sn_5$	2.5	0.24	$\frac{5}{2}$	1.79	0.88
$Pr_2Rh_3Sn_5$	-	-	4	2.19	1.56
$Nd_2Rh_3Sn_5$	-	-	$\frac{9}{2}$	2.30	1.18
$Gd_2Rh_3Sn_5$	10	1.74	$\frac{7}{2}$	2.08	1.8
$Tb_2Rh_3Sn_5$	6,4.3[a]	0.6	6	2.57	1.3
$Dy_2Rh_3Sn_5$	6,3.8[a]	0.75	$\frac{15}{2}$	2.77	1.9
$Ho_2Rh_3Sn_5$	5.6	1.8	8	2.83	2.25
$Er_2Rh_3Sn_5$	1.9	0.8	$\frac{15}{2}$	2.773	2.0
$Tm_2Rh_3Sn_5$	2.3	1.8	6	2.56	2.1

[a]Multiple transitions.

[b]Transition temperatures are determined from C_p data.

For all samples the high temperature regions of C_p data could be fitted to the expression,

$$C_p = \gamma T + \beta T^3, \tag{6}$$

where γ is due to the electronic contribution and β is due to the lattice contribution. From the β value, we can estimate the θ_D using the relation

$$\theta_D = \left(\frac{12\pi^4 N r k_B}{5\beta}\right)^{1/3}, \tag{7}$$

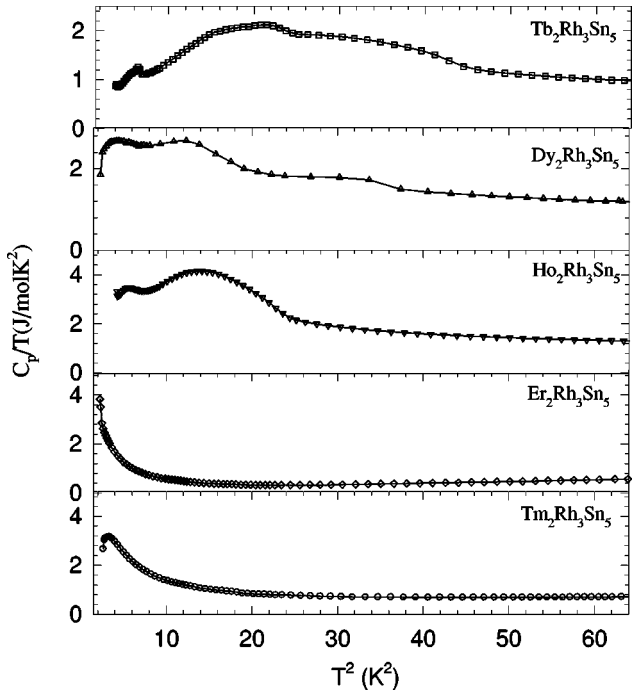

FIG. 8. Plot of low temperature C_p/T vs T^2 of $R_2Rh_3Sn_5$ (R =Tb, Dy, Ho, Er, and Tm).

where N is the Avogadro's number, r is the number of atoms per formula unit, and k_B is Boltzmann's constant. The θ_D values observed in this manner are included as final column of Table V for ease of comparison with the Debye temperatures derived from the high-temperature resistivity data. The estimated γ values for La and Y compounds are 10.5 mJ/mol K^2 and 3 mJ/mol K^2, respectively. The absence of superconductivity above 1.7 K in the latter compound could be attributed to the low value of γ.

From the Table VI, one can see that the estimated entropy at 35 K is very much less that value of $R\ln(2J+1)$ in all compounds containing magnetic rare-earth ion except for the case of Gd where they are close to each other. We attribute this to the contribution from the CEF levels and possible presence of magnetic correlations above T_N. We now briefly discuss the C_p data of every individual compound below. The temperature dependence of C_p from above 1.7–35 K of $Ce_2Rh_3Sn_5$ is shown in Fig. 7. The inset in Fig. 7 clearly shows the bulk magnetic ordering of Ce^{3+} moments at 2.5 K. This temperature is much lower than the value indicated ($\sim$5K) by the χ and ρ(T) measurements. The reason for this discrepancy is not understood at this moment. The reduction in the entropy value at 35 K compared with the expected value (see Table VI) implies contribution from CEF levels as well as Kondo effect as seen from the resistivity data. The extrapolated electronic heat-capacity coefficient (γ) has value of 150 mJ/Ce mol K^2 which classifies $Ce_2Rh_3Sn_5$ as a moderate heavy-electron antiferromagnet.

The temperature dependence of C_p from 2–35 K of $Pr_2Rh_3Sn_5$ in the same figure shows no anomaly around 2.5 K where one has observed a change in $\rho(T)$ implying that there is no bulk magnetic ordering in this sample down to 2 K. The magnetic contribution to the heat capacity (not shown here) obtained from subtracting the lattice part shows a broad hump around 10 K. This could be a Schottky anomaly arising from the contribution of the crystal field levels of Pr^{3+} ion. Similar behavior has been observed in $Pr_2Rh_3Si_5$,[24] where we have used a singlet ground state and a doublet excited state for CEF levels to explain the data. Inelastic neutron-scattering measurements will be useful here to directly estimate the CEF splitting. The temperature dependence of C_p from 3–35 K of $Nd_2Rh_3Sn_5$ (Fig. 7) also shows no bulk magnetic ordering in this temperature range which is consistent with χ and ρ measurements. The low value of the estimated entropy (see Table VI) at 35 K could arise due to the existence of CEF contributions and short-range magnetic correlations. The inset shows the plot of C/T vs T^2 from which we could estimate the Sommerfeld coefficient γ as 300 mJ/Nd mol K^2. A large value of γ can also be accounted for either by the CEF effects or by short-range magnetic correlations. Inelastic neutron measurements will help us to resolve this issue as in the case of $Pr_2Rh_3Si_5$. The C_p from 2–35 K of $Gd_2Rh_3Sn_5$ in the same figure shows a large jump at 10 K ($\Delta C = 16$ J/mol K) which clearly indicates a bulk magnetic ordering of Gd^{3+} spins in this sample. The data also show a shoulder at 4 K which can be associated with the moment reorientation effects. However, at this stage the above statement is only a conjecture. The normalized total entropy below T_N is found to be 1.8 R. This value of is still less than the expected value of 2.08 R (see Table V) which implies the existence of short range magnetic correlations above T_N.

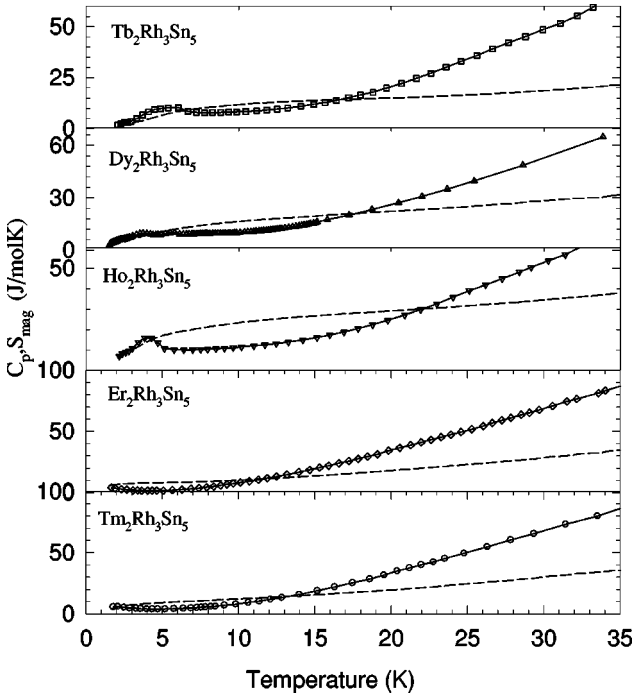

FIG. 9. Temperature dependence of the heat capacity (C_p) of $R_2Rh_3Sn_5$ (R=Tb, Dy, Ho, Er, and Tm). The calculated values entropy S_{mag} (after the subtraction of the lattice contribution from C_p) are also given.

From Figs. 8 and 9, the C_p data of $Tb_2Rh_3Sn_5$ and $Dy_2Rh_3Sn_5$ exhibit two transitions while one can only discern a single transition in the other three compounds with strong CEF. The total entropy below T_N is found to be close to the value $R\ln 2$ which indicates that the magnetic ground state is a doublet in these compounds. In the case of $Er_2Rh_3Sn_5$, the onset of magnetic ordering is observed at 2 K. However, we could not establish the complete transition since the transition occurs at a temperature which is below 2 K. The relaxation time is also quite large so as to prevent any cooling below 2 K. However, the C/T vs T^2 plot nearly indicates magnetic ordering of Er^{3+} spins below the onset at 2 K. Although we could establish bulk magnetic ordering of Tm^{3+} ions at 2.3 K in $Tm_2Rh_3Sn_5$ we could not distinguish the superconducting transition since the said transition occurs at a temperature which is near to the antiferromagnetic ordering at 2.3 K.

IV. DISCUSSION

In this section we will make an attempt to understand the temperature dependence of measured physical properties and the models which we have to used to understand their behavior. We begin with the results obtained for the resistivity behavior at low and high temperatures. From the Table IV, we infer that most of the samples have resistivity values typical of rare-earth intermetallic compounds at low temperatures and the resistivity of the rare-earth compounds containing magnetic elements show T^2 dependence suggesting the dominance of spin fluctuations at these temperatures. The

only exceptions are the resistivities of $Ce_2Rh_3Sn_5$, $Er_2Rh_3Sn_5$, and $Tm_2Rh_3Sn_5$. In the case of Ce compound we see a heavy-fermion behavior and the expected T^2 dependence might occur at very low temperature (below 1 K). However, the $T^{2.5}$ and $T^{1.5}$ dependence of $\rho(T)$ dependence at low temperatures of $Er_2Rh_3Sn_5$ and $Tm_2Rh_3Sn_5$ is quite puzzling and not understood at the present moment. As we have seen before, although the resistivity of $Gd_2Rh_3Sn_5$ shows a T^2 dependence from degrees above T_N and 40 K, the ρ exhibits a $T^{1/2}$ dependence between 1.5 K and T_N. Such a fractional dependence of ρ on T can be understood in terms of the elastic scattering of conduction electrons by critical spin fluctuations which will be present as one approaches T_N. These fluctuations cause large angle scattering of conduction electrons even below T_N and this implies large momentum transfer between conduction electrons and the scattering system. This momentum is of course limited by the momentum cutoff which is 2 k_F where k_F is the Fermi wave vector. In the case of antiferromagnetic metals, when T_N is approached from above, the large q fluctuations (where **q** is the fluctuation wave vector of the spin system) grow since the antiferromagnetic order is associated with the large reciprocal magnetic lattice vector **Q**. As T increases above T_N, the small-q fluctuations grow at the expense of large-q fluctuations resulting in the decrease of resistivity with increase of temperature. Below T_N the reverse is true and hence the resistivity decreases as $T^{1/2}$ leading to a maximum value of resistivity at T_N. In the case of $Gd_2Rh_3Sn_5$, we do see the $T^{0.5}$ dependence ($1.5<T<10$ K) but we do not see the maximum in ρ due to the additional contribution to ρ from electron-phonon interaction. However, the explanation of the T^2 dependence of ρ above T_N is only a conjecture since the theory of critical scattering is developed for $\rho(T)$ behavior near the phase transition. But such a dependence has been seen in the resistivity of a single crystal of Dy at a temperature far away from the antiferromagnetic transition in an earlier study.[25] Clearly, studies on a single crystal of $Gd_2Rh_3Sn_5$ are required for further analysis.

Although we could fit the high-temperature dependence of ρ to the parallel resistor model (see Table V) successfully, the θ_D values obtained from such fits do not agree with those obtained from heat-capacity data for almost all compounds (magnetic or nonmagnetic) of the series $R_2Rh_3Sn_5$. One of the reasons could be due to anharmonic contribution which is not considered in the parallel resistor model. The values of ρ_{max} also vary considerably across the series. More investigations are clearly needed here to understand the transport properties of these compounds at high temperatures.

We now turn our attention to some of the systematic trends observed in the magnetic properties at low and high temperatures. The values of the ordering temperature T_N, entropy $S(T_N)/R$, J, $\ln(2J+1)$ and $S(35\ \mathrm{K})/R$ are given in Table VI. We have determined the transition temperatures using ρ, χ, and C_p measurements (see Table III). In most cases they agree with each other. However, notable differences are seen in compounds with Ce, Tb, and Dy. For the purpose of analysis, we have assumed that the temperatures obtained from C_p data are the true transition temperatures. In general, the antiferromagnetic ordering temperature T_o is given by[26]

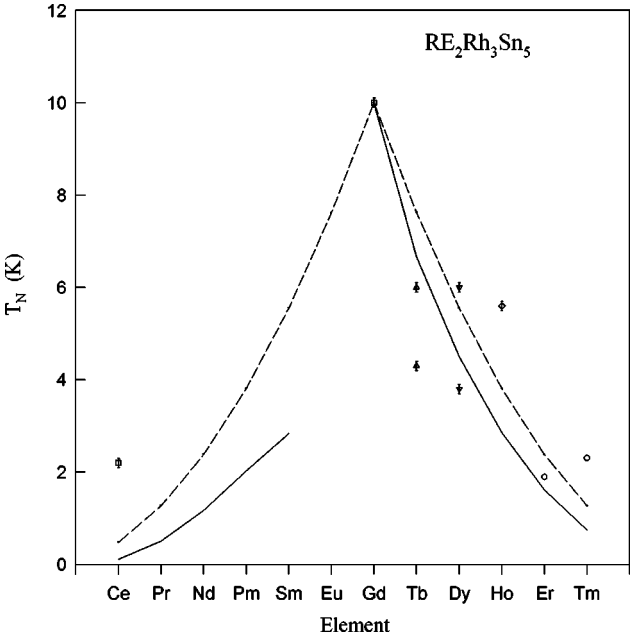

FIG. 10. Plot of the ordering temperatures of the compounds of the series $R_2Rh_3Sn_5$ (R=Ce, Pr, Nd, Gd, Tb, Dy, Ho, Er, and Tm). The dashed lines represent scaling law where only spin quantum number S is used whereas the solid lines are for scaling law using total quantum number J (de Gennes scaling, see text for details).

$$T_o=\theta_p=\frac{3\pi n^2}{k_B E_F}J_{sf}^2(g_J-1)^2J(J+1)$$
$$\times\Sigma_{i\neq 0}F(2k_FR_{Oi})\cos(\mathbf{k}_o\cdot\mathbf{R}_{Oi}), \qquad (8)$$

where E_F is the Fermi energy, J_{sf} is the exchange integral, $\mathbf{k}_o$ is the propagation vector of spins, $\mathbf{R}_{Oi}$ is the distance between the central ion O with its i nearest neighbors, and n is the density of conduction electrons. $F(x)$ is the Ruderman-Kittel-Kasuya-Yosida (RKKY) interaction and it is given by

$$F(x)=\frac{[\sin(x)-x\cos(x)]}{x^4}. \qquad (9)$$

This implies that the magnetic ordering temperatures for a series of isostructural and isoelectronic metals are expected to scale (de Gennes scaling[27]) as $(g_J-1)^2\ J(J+1)$ where g_J is the Lande g factor and J is the total angular momentum of the local moment. If the angular momentum is quenched then T_Ns are expected to scale as $S(S+1)$.

The solid line in Fig. 10 represents the ordering temperatures expected for various compounds based on heavy rare-earth elements of the series $R_2Rh_3Sn_5$ normalized to the observed ordering temperature (highest one) of $Gd_2Rh_3Sn_5$ since S is a good quantum number in this case. The dashed line is obtained by similar normalization to the observed ordering temperature of $Gd_2Rh_3Sn_5$ and gives the ordering temperatures for the case where J is the good quantum number. From the Fig. 10, it is evident that the ordering temperatures of the compounds do not follow the de Gennes scaling $(g_J-1)^2\ J(J+1))$. The fact is that many of them do not follow the de Gennes scaling. This implies that the main interaction leading to the magnetic transitions in this series may not be due to RKKY interaction. All compounds containing the magnetic rare-earth elements (other than R

=Gd) approximately show an entropy change of $R \ln 2$ at T_N which implies a doublet ground state. Large contributions from the CEF are evident since the full entropy is not released at 35 K in all compounds except in the case of $Gd_2Rh_3Sn_5$ where there is no CEF contribution. It is well known that the CEF (in the case of doublet ground state) can enhance the magnetic transition temperature[28] and this could in principle account for the difference between the observed data and de Gennes scaling. However, it can also suppress the transition when singlet ground states are involved and the exchange interaction is weak. If we add the CEF terms to the exchange Hamiltonian, one can write an expression for the transition temperature as[28]

$$T_o = \frac{2G(g_J-1)^2 \Sigma_{J_z} J_z^2 \exp(-3B_2^o J_z^o/T_N)}{\Sigma_{J_z}[\exp(-3B_2^o J_z^2/T_N)]}, \qquad (10)$$

where G is the exchange constant for the $4f$ atoms and B_2^o is the crystal field parameter. Since Gd is an S-state ion, its ordering temperature can be used to fix the value of the exchange constant. However, we find that the calculated values of T_N are lower than the observed values if one uses the B_2^o values from our preliminary CEF analysis. In the orthorhombic symmetry of $R_2Rh_3Sn_5$, the crystal field is characterized by seven real parameters, which includes four cubic parameters. The limited experimental data prevents us from the independent determination of all the crystal-field parameters unambiguously. In order to keep the number of parameters to a minimum, we retained the fourth-order cubic terms and second-order axial distortion term only. Details of the crystal-field analysis will be published elsewhere.[29] Hence we believe that the reason for the discrepancy between observed T_N and that found from de Gennes scaling is not due to CEF.

In the case of $4f$ systems, there is a large spin-orbit coupling because the orbital contribution to the magnetic moment is only partially quenched by the crystal field. This means, because of the highly directional nature of the $4f$ orbitals, that the exchange between two f ions may be expected to contain certain anisotropic terms which depends on the angles between the magnetic moments and the crystallographic axes as well as on the relative angle between the magnetic-moment vectors. The presence of such anisotropic interactions have been demonstrated by Birgeneau and others.[30] This anisotropic interaction causes the canting of the local moments only if the total symmetry is the same in the canted as well as uncanted state. The canting angle is usually of the order of the ratio of the anisotropic to isotropic exchange interaction. Such a theory in principle could account for the multiple transitions in systems where $L \neq 0$, such as, $Dy_2Rh_3Sn_5$ and $Tb_2Rh_3Sn_5$. Here we must also mention that the situation in $R_2Rh_3Sn_5$ is quite complicated due to the presence of eight rare-earth atoms in the unit cell with two rare-earth sites with different local symmetries. Single-crystal studies will be useful in this case and efforts to grow them are in progress.

V. CONCLUSION

To conclude, we have observed antiferromagnetic ordering in all compounds of the series $R_2Rh_3Sn_5$ containing magnetic rare-earth elements below 10 K. $Ce_2Rh_3Sn_5$ shows a Kondo-lattice behavior with antiferromagnetic ground state. The nonmagnetic sample $La_2Rh_3Sn_5$ exhibits superconductivity at 1.7 K whereas $Y_2Rh_3Sn_5$ remains normal down to 1.6 K. The magnetic ordering temperatures of heavy rare-earth compounds of the series $R_2Rh_3Sn_5$ (for examples R=Gd and Tb) are smaller than those of $R_2Fe_3Si_5$ system[8,9] which could be ascribed to the reduction in the unit-cell volume (i.e., smaller distance between the rare-earth ions) of the latter compared to that of the former. Although there is considerable increase in conduction electron density in the $R_2Rh_3Sn_5$ series compared to that of the $R_2Rh_3Si_5$, the unit-cell volume of $R_2Rh_3Sn_5$ is larger than that of $R_2Rh_3Si_5$. Hence, the distance between the rare-earth atoms is large enough so that the exchange interaction between the magnetic rare-earth atom and the conduction electrons is weaker than that of $R_2Rh_3Si_5$ series. That is why antiferromagnetic ordering temperatures in $R_2Rh_3Sn_5$ are comparable to that of $R_2Rh_3Si_5$ series.[31] Even though the magnetic ordering in $Gd_2Rh_3Sn_5$ can be understood in terms of usual second-order phase transition, we do not know whether the unusual $T^{1/2}$ dependence of ρ below T_N can be really due to critical scattering effects as we have discussed before. At present it is a puzzle that warrants more detailed investigations of its transport properties near T_N as well as down to very low temperatures (<1K). Finally, the observation of coexistence of magnetism and superconductivity in $Tm_2Rh_3Sn_5$ is unusual and such behavior has been observed only in $TmNi_2B_2C$.[32,33] It must be recalled here that superconductivity and antiferromagnetism have been observed in $Tm_2Fe_3Si_5$,[10] where the compound makes a transition to normal state (reentrant state) at the antiferromagnetic transition unlike the coexistence of two phase transition below 1.5 K in $TmNi_2B_2C$. Hence, in view of the reasons stated above, $Tm_2Rh_3Sn_5$ certainly deserves further investigations, preferably on single crystals.

[1] P. Rogl, in *Handbook of Physics and Chemistry of Rare Earths*, edited by K.A. Gschneidner, Jr. and L. Eyring (Elsevier Science Publishers, Amsterdam, 1984), Vol. 7, pp. 1-264.

[2] J. Leciejewicz and A. Szytula, in *Handbook of Physics and Chemistry of Rare Earths*, edited by K.A. Gschneidner, Jr. and L. Eyring (Elsevier Science, Amsterdam, 1989), Vol. 12, p. 133.

[3] H.F. Braun, J. Less-Common Met. **100**, 105 (1984).

[4] R.N. Shelton, in *Proceedings of the International Conference on Superconductivity in d- and f-band Metals*, edited by W. Buckel and W. Weber (Kernforshungszentrum, Karlsruhe, Germany 1982), p. 123.

[5] H.F. Braun, Phys. Lett. **75A**, 386 (1980).

[6] H.F. Braun, C.U. Segre, F. Acker, M. Rosenberg, S. Dey, and U. Deppe, J. Magn. Magn. Mater. **25**, 117 (1981).

[7] A.R. Moodenbaugh, D.E. Cox, and H.F. Braun, Phys. Rev. B **25**, 4702 (1981).

[8] C.B. Vining and R.N. Shelton, Phys. Rev. B **28**, 2732 (1983).
[9] H.F. Braun, in *Ternary Superconductors*, edited by G.K. Shenoy, B.D. Dunlap, and F.Y. Fradin (North-Holland, Amsterdam, 1980), p. 225.
[10] J.A. Gotaas, J.W. Lynn, R.N. Shelton, P. Klavins, and H.F. Braun, Phys. Rev. B **36**, 7277 (1987).
[11] S. Noguchi and K. Okuda, Physica B **194-196**, 1975 (1994).
[12] B. Chevalier, P. Lejay, J. Etourneau, M. Vlasse, and P. Hagenmuller, Mater. Res. Bull. **17**, 1211 (1980).
[13] P. Lejay, I. Higashi, B. Chevalier, J. Etourneau, and P. Hagenmuller, Mater. Res. Bull. **19**, 115 (1984).
[14] G. Venturini, M. Meot-Meyer, J.F. Mareche, B. Malaman, and B. Roques, Mater. Res. Bull. **21**, 33 (1986).
[15] N.G. Patil, K. Ghosh, and S. Ramakrishnan, Phys. Rev. B **52**, 9679 (1995).
[16] M. Meot-Meyer, G. Venturini, B. Malaman, J. Steinmetz, and B. Roques, Mater. Res. Bull. **18**, 1181 (1984).
[17] E. Parthe and B. Chabot, in *Handbook of Physics and Chemistry of Rare Earths* (Ref. 1, pp. 113-333.
[18] S. Ramakrishnan, S. Sundaram, R. S. Pandit, and Girish Chandra, J. Phys. E **18**, 650 (1985).
[19] M. Weger and I.B. Goldberg, in *Solid State Physics*, edited by H. Ehrenreich, F. Seitz, and D. Turnbull (Academic, New York, 1973), Vol. 28, p. 1.
[20] S. Ramakrishnan, K. Ghosh, and Girish Chandra, Phys. Rev. B **45**, 10 769 (1992).
[21] K. Ghosh, S. Ramakrishnan, and Girish Chandra, Phys. Rev. B **48**, 10 440 (1993).
[22] H. Wiesmann, M. Gurvitch, H. Lutz, A.K. Ghosh, B. Schwarz, M. Strongin, P.B. Allen, and J.W. Halley, Phys. Rev. Lett. **38**, 782 (1977).
[23] B. Chakraborty and P.B. Allen, Phys. Rev. Lett. **38**, 372 (1979).
[24] N.G. Patil and S. Ramakrishnan (unpublished).
[25] R.A. Craven and R.D. Parks, Phys. Rev. Lett. **31**, 383 (1973).
[26] D.C. Mattis, *Theory of Magnetism* (Harper & Row, New York, 1965).
[27] P.G. de Gennes, J. Phys. Radium **23**, 510 (1962).
[28] D.R. Noakes and G.K. Shenoy, Phys. Lett. **91A**, 35 (1982).
[29] N.G. Patil, Arvind D. Chinchure, S. Ramakrishnan, and V.R. Marathe (unpublished).
[30] R.J. Birgeneau, M.T. Hutchings, J.M. Baker, and J.D. Riley, J. Appl. Phys. **40**, 1070 (1969).
[31] N.G. Patil and S. Ramakrishnan, Physica B **237-238**, 597 (1996).
[32] H. Eisaki, H. Takagi, R.J. Cava, B. Batlogg, J.J. Krajewski, W.F. Peck, Jr., K. Mizuhaashi, J.O. Lee, and S. Uchida, Phys. Rev. B **50**, 647 (1994).
[33] R. Movshovich, M.F. Hundley, J.D. Thompson, P.C. Canfield, B.K. Cho, and A.V. Chubukov, Physica C **227**, 381 (1994).